



# Morphometric analysis of early Eocene *Corbisema* skeletons (Silicoflagellata) in Mors, Denmark

Hideto Tsutsui<sup>1,a</sup>, Richard W. Jordan<sup>1</sup>, Niichi Nishiwaki<sup>2</sup>, and Shiro Nishida<sup>3</sup>

<sup>1</sup>Department of Earth and Environmental Sciences, Faculty of Science, Yamagata University, 1-4-12 Kojirakawa-machi, Yamagata 990-8560, Japan

<sup>2</sup>Faculty of Social Science, Nara University, 1500 Misasagi-cho, Nara 631-8502, Japan

<sup>3</sup>Earth Science, Faculty of Education, Nara University of Education, Takabatake, Nara 630-8528, Japan

<sup>a</sup>current address: Marine Microorganism Ecology, Division of Marine Biology & Dynamics, Department of Fisheries, Faculty of Fisheries, Nagasaki University, Bunkyo-cho 1-14, Nagasaki 852-8521, Japan

**Correspondence:** Hideto Tsutsui (blacksand@mail.goo.ne.jp)

Published: 7 February 2018

**Abstract.** A two-dimensional morphometric programme, recently designed to measure fossil skeletons of the silicoflagellate genus *Corbisema*, was used to investigate specimens of the *C. apiculata*–*C. triacantha* complex found in a sample from the Fur Formation on the island of Mors, Jutland, Denmark. The semi-automated programme measured the lengths of the basal sides and radial spines, the basal side curvature, and the location of the pikes (if present) from a photographic database ( $N = 469$ ). As a result, two distinct morphological groups were revealed based on their radial spine length : basal side length ratio and the presence or absence of pikes: group A (ratio of 1 : 1.3, no pikes) and group B, with the latter subdivided into B1 (ratio of 1 : 7, with pikes) and B2 (ratio of 1 : 6, no pikes). Group A (*C. triacantha sensu lato*) possesses a small basal ring with relatively straight basal sides and long radial spines, while group B has a large basal ring with curved basal sides and short radial spines. In B1 specimens (*C. apiculata sensu stricto*) the pikes are positioned 0 to 1  $\mu\text{m}$  away from the junction point of the strut and basal ring. This would suggest that B1 double skeletons are likely to be in the Star-of-David configuration, while A and B2 double skeletons (which lack pikes) are likely to be in the corner-to-corner configuration. Compared with the previously published biometric studies of extant *Stephanocha* (*Stephanocha speculum* complex in the Southern Ocean and *S. medianocisol* in the Arctic Ocean), the results are somewhat different: although *C. triacantha sensu lato* (group A) is similar to the modern species of *Stephanocha*, the latter have smaller basal ring diameters, whereas specimens of *C. apiculata sensu lato* (types B1 and B2) have large basal rings. If their cell diameters are calculated, B1 is the largest, with *S. speculum* being the smallest – about half the size of B1. This could suggest that the relationship between radial spine length and mean basal ring size has shifted over geological time.

## 1 Introduction

Silicoflagellates are unicellular marine phytoplankton that are either motile (uniflagellate) and possessing an external basket-like siliceous skeleton or naked and amoeboid (Henriksen et al., 1993; Chang, 2015). According to Chang (2015), *Octactis pulchra* (cited therein as *Dictyocha octonaria*) has a complicated life cycle, in which the skeleton-bearing forms divide by simple binary fission either

forming two new identical daughter skeletons (after discarding the mother skeleton) or producing a daughter skeleton opposite the original mother skeleton before the separation of the two cells. Sometimes thinner skeletons have been observed in association with thicker skeletons (e.g. Marshall, 1934; Abe et al., 2015; Malinverno et al., 2016), and these are now thought to be the daughter and mother skeletons, respectively. However, this has not been supported yet by culture

observations. Although the existence of double skeletons has been known for almost 100 years (e.g. Gemeinhardt, 1930), and they were often illustrated as sketches in subsequent publications (e.g. Loeblich et al., 1968; Dumitrică, 1974), light and scanning electron micrographs of a wide range of both fossil and modern double skeletons were only documented recently by McCartney et al. (2014, 2015). This has led to the proposal that double skeleton configurations (corner-to-corner or Star-of-David) and the position of the pikes (if present) that hold the skeletons together may be useful in silicoflagellate taxonomy (Dumitrica, 2014; McCartney et al., 2015; Tsutsui and Jordan, 2016).

There is still an ongoing debate about the number of extant genera, with biologists often lumping them into one genus, *Dictyocha*, while palaeontologists often opt for two or three genera, *Dictyocha* and *Octactis* (e.g. Dumitrica, 2014) or with *Stephanocha* included (e.g. McCartney et al., 2014, 2015). Modern silicoflagellates are cosmopolitan, but their distribution can be roughly separated into warm water (*Dictyocha*), cold water (*Stephanocha*), and coastal (*Octactis*) regions (e.g. Ignatiades, 1970; Rigual-Hernández et al., 2010, 2016; Malinverno, 2010; Onodera and Takahashi, 2012; Abe et al., 2015). Taxonomic studies on fossil silicoflagellates have been largely related to biostratigraphic analyses, with little consideration about their morphologic plasticity (i.e. aberrants, morphometric data). This has led to morphologically similar forms being regarded as taxonomic synonyms or species complexes having long stratigraphic ranges. One such example is the *Corbisema triacantha–apiculata* complex. Hanna (1931) distinguished the two species as follows: *C. apiculata* has curved basal sides, short radial spines, and pikes attached to the junction point between the strut and the basal ring, and *C. triacantha* has linear basal sides, radial spines of the same length as the basal sides, and no pikes. Subspecific taxa of *C. triacantha* (including var. *apiculata*) have been recorded from the Cretaceous to the Holocene, with a range of morphologies. According to Loeblich et al. (1968) the type locality of *C. triacantha* is Maryland, USA and thus Miocene in age, while that of *C. apiculata* appears to be Mors and therefore early Eocene in age. Herein we regard some of our specimens as belonging to *C. triacantha sensu lato*, since it is beyond the scope of the present study to investigate its entire biostratigraphic range. In addition, given that Tsutsui and Jordan (2016) recognised pike and pikeless forms of *C. apiculata*, we have designated only the former specimens as *C. apiculata sensu stricto*, referring to both of them collectively as *C. apiculata sensu lato*.

Some studies have shown the usefulness of collecting morphometric information and producing computer programmes that can analyse large quantities of numerical or photographic data. One such programme that measures *Corbisema* skeletons has been published recently (Tsutsui and Jordan, 2016) and the preliminary measurement data showed therein revealed two morphologic groups within *Corbisema apiculata*. In the present study we further investigate the *C.*

*triacantha–C. apiculata* complex using the same programme in order to shed some light on the problems surrounding this taxonomic confusion.

## 2 Materials and methods

Sample E1758, labelled “Mors Dänemark Zementstein 2”, was obtained from the Friedrich Hustedt diatom collection housed at the Alfred Wegener Institute in Bremerhaven, Germany. The online database gives no indication as to where, when, and by whom the sample was collected. However, it is likely to be from a cement works on the island of Mors, Denmark (see Fig. S1 in the Supplement), which mined the Fur Formation, an interval known to contain silicoflagellates (Perch-Nielsen, 1976).

Subsamples of the Mors sample were strewn onto cover slips, dried on a hot plate and made into permanent mounts using Mountmedia (Wako Pure Chemical Industries, Ltd.) as a mountant, following the method outlined in Shiono and Jordan (1996). A total of 469 specimens were photographed and measured, which is statistically sufficient when the minor group is  $N > 20$  and is close to normal distribution (e.g. Takeuchi, 2011; Tsuzaki, 2011). An example of the three *Corbisema* forms investigated in the present study is shown in Fig. S2a, b and c in the Supplement.

Details of the photography and the semi-automated programme used to take skeletal measurements can be found in the online Supplement and are similar to those given in Tsutsui and Jordan (2016).

## 3 Results

### 3.1 Photographic database

During this study, 469 specimens (i.e. individual skeletons) of the *Corbisema triacantha–apiculata* complex were photographed and measured. Based on the separation criteria of Hanna (1931), two groups were recognised and identified; group A belongs to *Corbisema triacantha sensu lato* (Fig. S2a, Plate 1), while group B represents *C. apiculata sensu lato*. However, in this study (as in Tsutsui and Jordan, 2016), there were two types within group B, B1 with pikes (Fig. S2b, Plate 2) and B2 without pikes (Fig. S2c, Plate 3). The number of specimens for each group and/or type was 289 (A), 153 (B1), and 27 (B2).

### 3.2 Primary measurements

The primary measurements of the skeletal parts (radial spine, basal side, strut length, basal ring corner–strut attachment position distance) of all 469 specimens of the *Corbisema triacantha–apiculata* complex are shown in Fig. 1a–d and summarised in Table 1, with the strut–pike distance provided for the 153 B1 specimens only (Fig. 1e). The radial spine length ranges from 3–49  $\mu\text{m}$  with a mean of 17  $\mu\text{m}$ , and the

### *Corbisema* group A

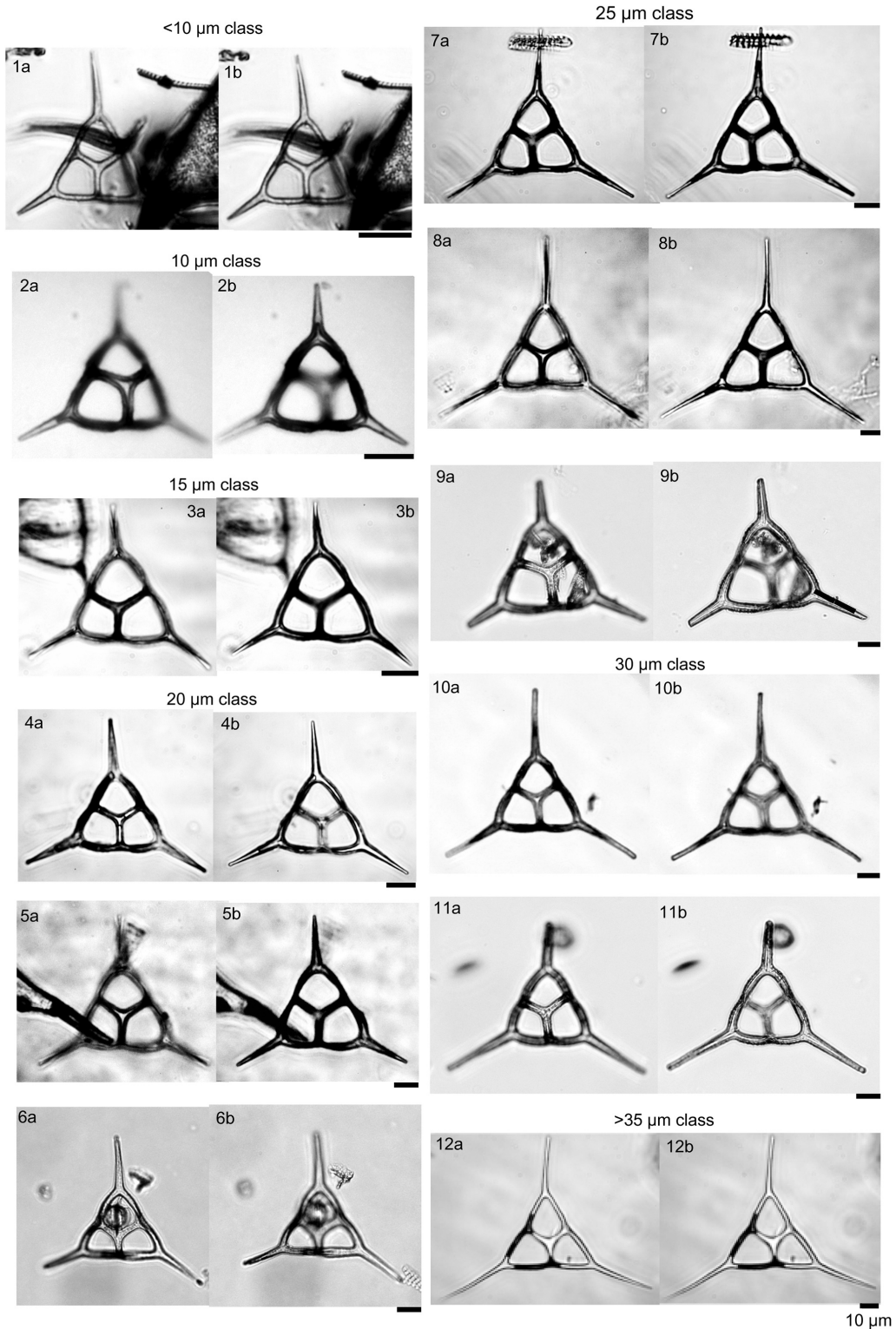


**Plate 1.** *Corbisema triacantha sensu lato* (group A) with photographs separated into class sizes of radial spine length.

### *Corbisema* type B1

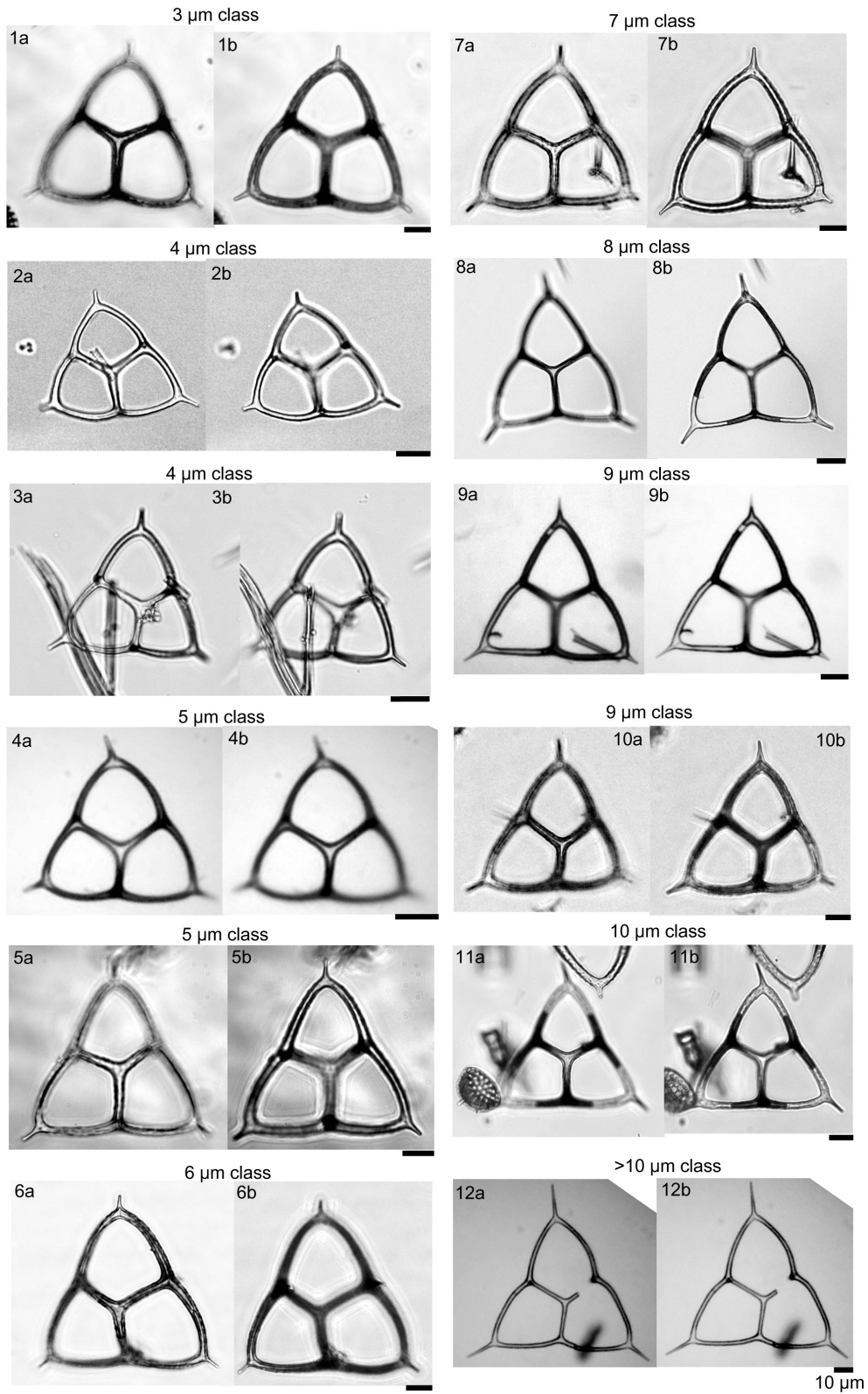


**Plate 2.** *Corbisema apiculata sensu stricto* (group B, type B1) with photographs separated into class sizes of radial spine length.

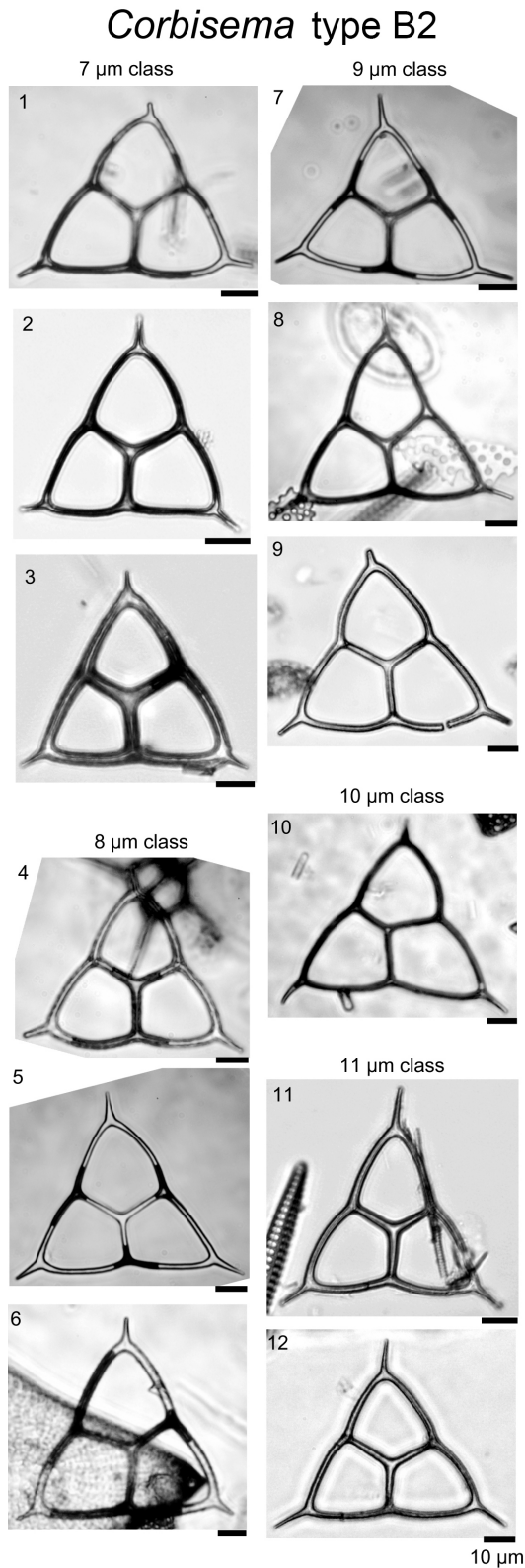


**Plate 3.** *Corbisema apiculata sensu lato* (group B, type B2) with photographs separated into class sizes of radial spine length.

basal side from 15–74  $\mu\text{m}$  with a mean of 38.3  $\mu\text{m}$ . If the data on radial spine (Fig. 2a) and basal side (Fig. 2b) lengths for group A and types B1 and B2 are presented, the two groups can be clearly separated, while the two types overlap. The peak of the pike position is 0–1  $\mu\text{m}$ , which is slightly away from the strut position, while the maximum distance is 4  $\mu\text{m}$  away from the strut, with a mean of 0.71  $\mu\text{m}$  (Table 1 and Fig. 1e). Only approximately 25% (153 of 469) of the total *Corbisema triacantha-apiculata* assemblage had pikes.

A database of theoretical skeletons can be produced for *C. triacantha* in which basal side length increases on the y axis and radial spine length on the x axis. If the data of measured specimens are inserted into the plot (as bold skeletons) with their relative abundances, then it is clear that they occupy the bottom left-hand quadrant (Fig. 3). In other words, few or no giant specimens were found (large basal rings and very long spines) with one extreme skeletal part (very long spines and small basal rings or large basal rings with small spines). The same pattern was seen in *C. apiculata* (B1 data only) for which the measured data plotted in the left-hand quadrant (Fig. 4).

Since all the elements on individual *Corbisema* specimens were measured, we have plotted the maximum and minimum radial spine lengths (Fig. 5a) and basal side lengths (Fig. 5b) for groups A and B. This clearly shows that both radial spine lengths and basal side lengths are variable on a single skeleton.

The basal ring diameter for *Corbisema triacantha* and *C. apiculata* (both types) was plotted against radial spine length, along with the data from two other published species (the *Stephanocha speculum* complex and *S. medianocisol*), as a scattergram (Fig. 6a) and with ranges and error bars (Fig. 6b). *Corbisema triacantha* was clearly separated from the others, while the two types of *C. apiculata* plotted on top of each other, and the two *Stephanocha* species were close to each other. Herein we refer to *S. speculum* as a species complex given the fact that the type locality is Oran in Algeria (Miocene in age) according to Loeblich et al. (1968), and modern *Stephanocha speculum* is sometimes separated into numerous subspecific taxa (e.g. Malinverno, 2010).

### 3.3 Simple statistics

All measured skeletal parts show a wide range in kurtosis and skewness. When the data of radial spine and basal side lengths are plotted they appear to show a roughly bimodal distribution (Fig. 1). The bimodal boundary of radial spine length is 15  $\mu\text{m}$  (Fig. 1a), and the basal side length is 48–53  $\mu\text{m}$  (Fig. 1b). The distance between the basal ring corner and the attachment point of struts on the basal side (e.g. the distance between B1 and R1 in Fig. S2d) also indicated a roughly bimodal distribution. The bimodal distribution of strut length is also affected by the basal side length, but the radial spine kurtosis value in Table 1 is  $-1.13$ , which sug-

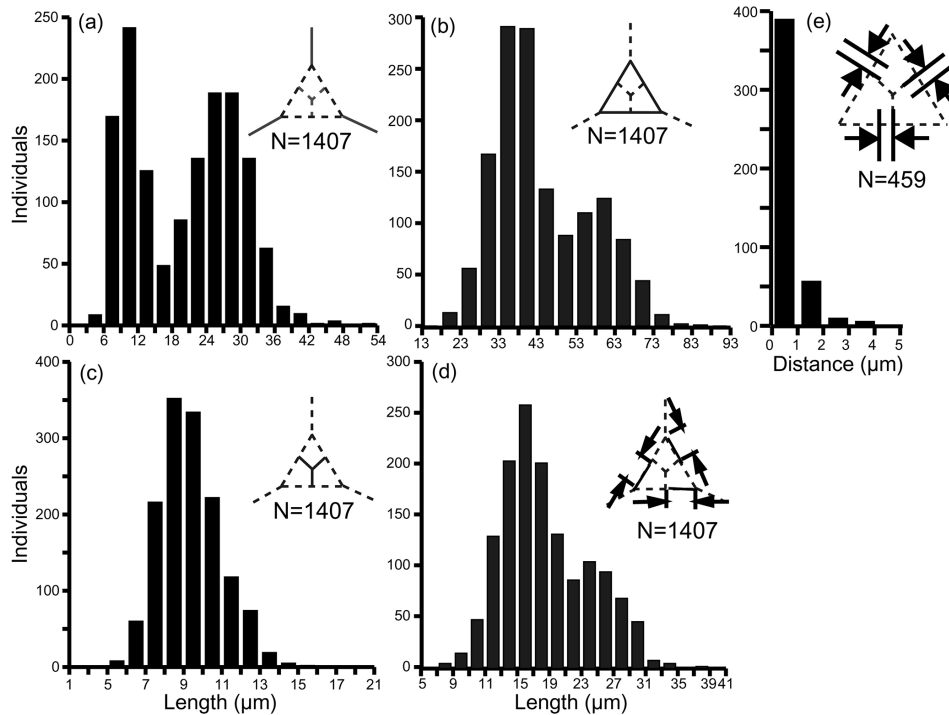


**Figure 1.** Primary measurement histogram of all skeletal parts; (a) radial spine, (b) basal side, (c) strut length, (d) the distance from the basal ring corner to the strut attachment position, and (e) strut–pike distance (B1 data only, as other forms lacked pikes). (a–d) Based on three skeletal parts of 469 specimens ( $N = 1407$ ). (e) Based on three skeletal parts of 153 specimens ( $N = 459$ ).

**Table 1.** Summary of the measurement data for each skeletal part, including the distance between the basal corner to strut (e.g. B1 to R1 in Fig. S2d), for which the total number of specimens is 469 (i.e. groups A and B combined), and the distance from the pike to the strut, for which the total number of pike-bearing specimens is 153 (i.e. B1 only). SD: standard deviation.

	Radial spines	Basal sides	Struts	Distance from basal corner to strut	Distance from pike to strut
Min ( $\mu\text{m}$ )	3	15	3	6	0
Max ( $\mu\text{m}$ )	49	79	29	38	5
SD ( $\mu\text{m}$ )	9.1	11.9	3.3	5.5	0.95
Mean ( $\mu\text{m}$ )	17.9	39.4	12.2	19.1	0.81
Variance	83.28	143.69	10.69	30.09	0.91
Skewness	0.07	0.62	0.57	0.53	1.39
Kurtosis	-1.13	-0.43	0.59	-0.33	2.20
				( $N = 469$ )	( $N = 153$ )

gests that radial spines, basal sides, and struts have a bimodal or trimodal normal distribution.

The base of the normal distribution of radial spine length or basal side length is very wide (Fig. 1a and b), with the first and second peaks of radial spine length being 9–12  $\mu\text{m}$  and 24–30  $\mu\text{m}$ , respectively, while the first and second peaks of basal side length are 33–43 and 58–63  $\mu\text{m}$ , respectively.

## 4 Discussion

### 4.1 Separation of taxa by morphometrics

In this study, the lengths of radial spines and basal sides and the presence or absence of pikes have been used to distinguish previously confused taxa within the *Corbisema triacantha–apiculata* complex. Histograms of radial spine length (Fig. 2a) and basal side length (Fig. 2b) clearly separated the individuals into two groups: group A with long spines and short basal sides and group B with short spines and long (and curved) basal sides. However, 27 out of 180

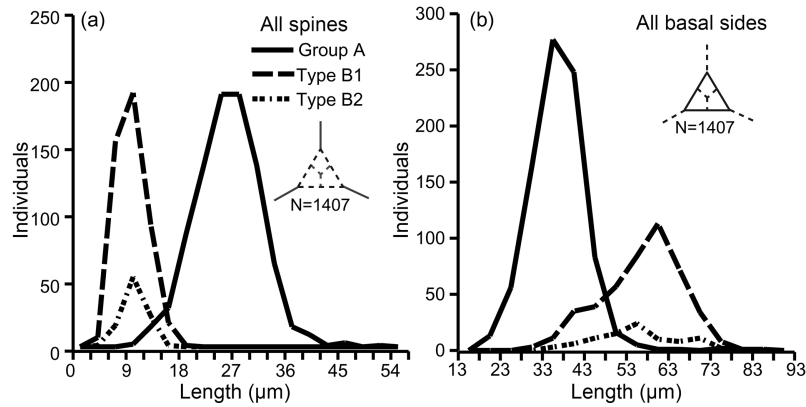


**Figure 2.** Separation of groups A and B (subdivided into B1 and B2) using (a) radial spine length and (b) basal side length. Based on three skeletal parts of 469 specimens ( $N = 1407$ ).

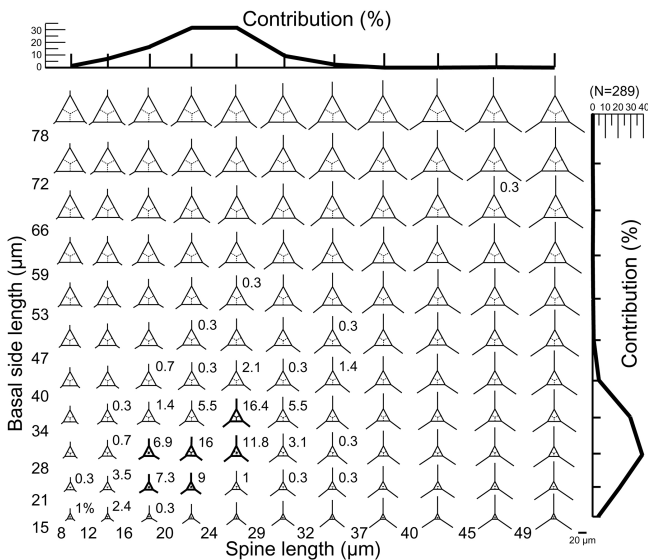


**Figure 3.** A plot of theoretical skeletal forms of *Corbisema* group A (*C. triacantha*) exhibiting a range of basal ring sizes and radial spine lengths, with bold skeletal forms representing those found in this study. The relative percentage of each form and the total contributions with respect to basal side length (vertical axis) and spine length (horizontal axis) are indicated on the plot. The scale bar is 20 µm. Based on the total number of measured specimens (group A;  $N = 289$ ).

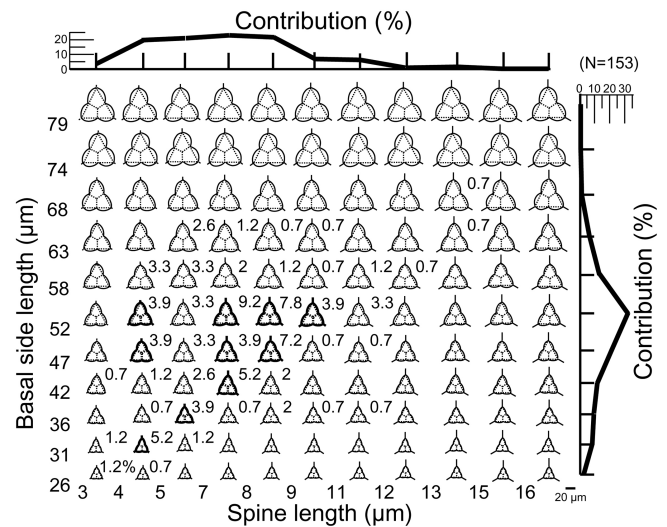


**Figure 4.** A plot of theoretical skeletal forms of *Corbisema* type B1 (*C. apiculata*) exhibiting a range of basal ring sizes and radial spine lengths, with bold skeletal forms representing those found in this study. The relative percentage of each form and the total contributions with respect to basal side length (vertical axis) and spine length (horizontal axis) are indicated on the plot. In order to accentuate the curvature of the basal ring, dotted lines on each image represent a mathematically perfect triangle. The scale bar is 20 µm. Based on the total number of measured specimens (type B1;  $N = 153$ ).

group B specimens lacked pikes, so these were treated as type B2, with those bearing pikes named type B1. Figures 3 (group A) and 4 (type B1) showed that the degree of variability in the two more common morphologies was relatively constrained to the bottom left-hand quadrant. Based on the criteria proposed by Hanna (1931), two of the morphological entities can be identified: group A is *Corbisema triacantha sensu lato*, while type B1 is *C. apiculata*. However, the identity of type B2 (which lacks pikes but is otherwise identical to type B1) is uncertain at present. Indeed, the histograms

of radial spine (Fig. 2a) and basal side (Fig. 2b) lengths and the plots of maximum–minimum basal side length and spine length (Fig. 5) failed to separate B1 from B2 specimens, leaving the presence or absence of pikes as the sole distinguishing characteristic.

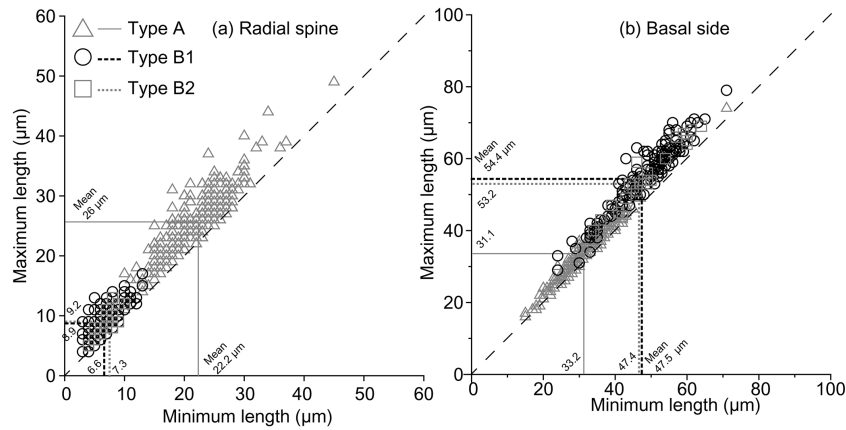


**Figure 5.** Plots of maximum and minimum radial spine length (a) and basal side length (b). The dashed line represents equality; i.e. lengths are equal on the same skeleton. Consequently, almost all of the *Corbisema* observed in this study had unequal radial spine lengths and basal sides. *Corbisema triacantha sensu lato* is group A (triangle) and *C. apiculata sensu lato* is group B, with the latter subdivided into B1 (circle) and B2 (square); *C. apiculata sensu stricto* is B1.

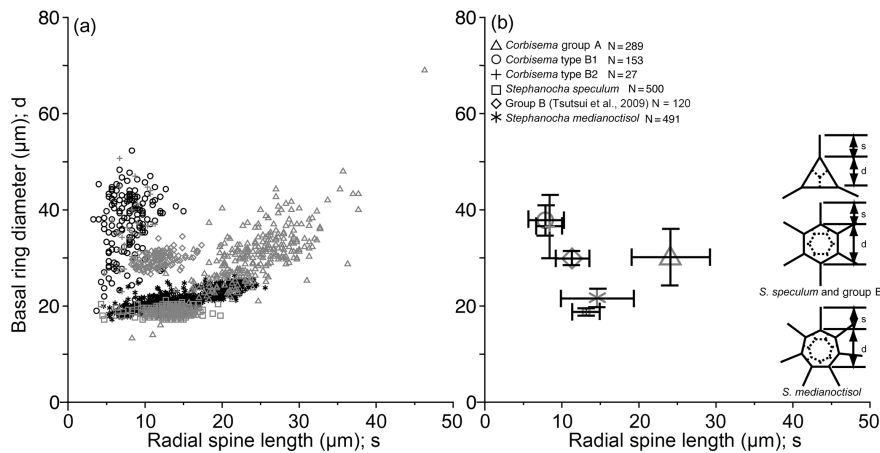


**Figure 6.** Plots of radial spine length vs. basal ring diameter showing the morphometric data of *Corbisema triacantha sensu lato* (group A) and *C. apiculata sensu lato* (group B, subdivided into B1 and B2), the extant *Stephanocha speculum* complex and group B in the Southern Ocean (from Tsutsui et al., 2009), and *S. medianoctisol* in the Arctic Ocean (from Tsutsui and Takahashi, 2009) as (a) a scattergram and (b) mean lengths with standard deviation (error bars). Data based on individual specimens not skeletal parts.

#### 4.2 Potential and observed *C. triacantha* and *C. apiculata* skeletons

Figure 3 represents a series of potential skeletal images for *Corbisema triacantha* (group A) based on increasing basal side length and increasing radial spine length. The most common forms have a basal side length of 28–40  $\mu\text{m}$ , a radial spine length of 20–29  $\mu\text{m}$ , and represent about 32 % of the total *C. triacantha* assemblage. Extreme skeletons were largely absent in our study, i.e. with short basal sides but long spines (basal side length 15–21  $\mu\text{m}$ , spine length > 49  $\mu\text{m}$ ) or long basal sides and short spines (basal side length 72–78  $\mu\text{m}$ , spine length 8–12  $\mu\text{m}$ ). In fact, most observed skeletons plot in the left-hand quadrant, suggesting that the skeletal dimensions of *C. triacantha* are relatively constrained.

Figure 4 represents a series of potential skeletal images for *Corbisema apiculata* (type B1 only) based on increasing basal side length and increasing radial spine length. The most common forms have a radial spine length of 7–9  $\mu\text{m}$ , a basal side length from 47–58  $\mu\text{m}$ , and represent about 23 % of the total *C. apiculata* assemblage. Extreme skeletons were largely absent in our study, i.e. with short basal sides but long spines (basal side length 26–52  $\mu\text{m}$ , spine length > 12  $\mu\text{m}$ ) or long basal sides and short spines (basal side length 68–79  $\mu\text{m}$ , spine length < 5  $\mu\text{m}$ ). The curvature becomes conspicuous when the basal side is > 74  $\mu\text{m}$ .

In *C. triacantha* and *C. apiculata* the skeletal shape is an isosceles (not equilateral) triangle in which one of the radial spine lengths is slightly longer than the other two (Fig. 5a) and one of the basal sides is slightly shorter (Fig. 5b). This

is similar to other fossil species such as *Corbisema hastata* and *Mesocena apiculata* (e.g. Loeblich et al., 1968; Tappan, 1980; Perch-Nielsen, 1985). In addition, other genera (such as *Stephanocha*, *Octactis*, and *Dictyochoa*) also possess one or two radial spines of unequal length, whereby in the case of two spines they are opposing (Bukry and Foster, 1973; Malinverno, 2010; Chang, 2015), resulting in bilateral rather than radial symmetry.

#### 4.3 Morphometric comparison between fossil *Corbisema* and living *Stephanocha*

*Corbisema triacantha* and *C. apiculata* can be easily separated by their radial spine length and basal side length. However, types B1 and B2 can only be distinguished by the presence or absence of pikes. The correlation coefficients between the radial spine length and basal side length are 0.7 (probability < 1 %) for *C. triacantha*, 0.47 (probability < 1 %) for *C. apiculata* (B1 only), and 0.44 for type B2. The mean radial spine length vs. basal side length ratio in *C. apiculata* (B1 only) is 1 : 7 (min. 1 : 3, max. 1 : 13) and for type B2 1 : ~ 6 (min. 1 : 5.5, max. 1 : 12).

Morphometric studies have concluded that the basal ring diameter is a useful index for both fossil and modern silicoflagellates (e.g. Kitchell, 1983; Poelchau, 1976; Tsutsui et al., 2009; Tsutsui and Takahashi, 2009; Malinverno, 2010) and can be closely approximated to cell size, as the living cell resides inside the skeletal area. Thus, it is natural to assume that recent silicoflagellates also inherited these skeletal characteristics from fossil silicoflagellates. Figure 6 compares the mean radial spine length with mean basal ring diameter of two *Corbisema* spp. (*C. triacantha* and *C. apiculata*) and two *Stephanocha* spp. (the *S. speculum* complex and *S. medianoetisol*). The biometric data for modern *S. speculum* and *S. medianoetisol* were re-measured from the datasets of Tsutsui et al. (2009), and Tsutsui and Takahashi (2009). As a result, *C. triacantha* and *C. apiculata* are clearly distinguished from each other (although types B1 and B2 are not), and the two *Stephanocha* spp., with their short radial spine length and small basal ring diameter, cluster together but are clearly separable from the *Corbisema* spp. The ratio of mean basal ring diameter to mean radial spine length of these taxa can be arranged from largest to smallest: group B in Tsutsui et al. (2009) (5.5), *Corbisema apiculata* type B2 (5.1), type B1 (4.5), *S. medianoetisol* in the Arctic Ocean (1.6), *S. speculum* (1.5), and *Corbisema triacantha* (1.3). Roughly, their cell size can also be sorted from largest to smallest by mean basal ring diameter: *Corbisema apiculata* type B1 (37 µm), B2 (36 µm), *C. triacantha* (30 µm), group B in Tsutsui et al. (2009) (30 µm), *S. medianoetisol* (21 µm), and *S. speculum* (19 µm). So the cells of modern silicoflagellates appear to be smaller than their fossil counterparts. Of course, more data are needed to determine whether this trend is real or not. In that respect, studies need to be conducted on other *Corbisema* species to see if there is an intrageneric trend;

*Corbisema* first appeared in the Cretaceous and disappeared in the late Miocene (e.g. Perch-Nielsen, 1985; McCartney et al., 2010). There are many examples of body mass downsizing in vertebrates, e.g. groundfish (Shackell et al., 2009), dinosaurs to birds (Chiappe, 2009), dinosaurs (Benton et al., 2010), and lizards (Pérez-Méndez et al., 2015), and similar trends have been recognised in various microfossil groups, such as coccolithophores (e.g. Young, 1990; Henderiks and Pagani, 2008) and diatoms (e.g. Suto, 2006; Cortese et al., 2012).

## 5 Conclusions

1. Early Eocene specimens of the *Corbisema triacantha*–*apiculata* complex from Mors can be separated into two morphological groups (A and B) using a morphometric programme specifically designed for *Corbisema* skeletons. In particular, radial spine and basal side lengths and basal ring diameter proved useful characteristics for separating these taxa, with the latter group further subdivided into types B1 and B2 based on the presence or absence of pikes, respectively.
2. Two of these morphologies can be identified as *C. triacantha sensu lato* (group A) and *C. apiculata sensu stricto* (type B1) based on the criteria of Hanna (1931).
3. Preliminary data on the ratio of basal ring diameter to radial spine length suggest that cells of fossil silicoflagellates were larger than their modern counterparts, although morphometric data on more taxa, particularly of the long-ranging genus *Corbisema*, are needed.

**Data availability.** Please see the Supplement for further information. The two files 1\_SILICO and 2\_SILICO contain the new data in this paper. Data from other papers used in comparison (e.g. Tsutsui et al., 2009; Tsutsui and Takahashi, 2009) are not provided here.

**Supplement.** The supplement related to this article is available online at: <https://doi.org/10.5194/jm-37-283-2018-supplement>.

**Competing interests.** The authors declare that they have no conflict of interest.

**Acknowledgements.** We would like to thank Friedel Hinz (Friedrich Hustedt Diatom Study Centre, Alfred Wegener Institute; AWI) for providing the Mors sample used in this study. At INA15 (Bohol, Philippines), Elisa Malinverno (Department of Earth and Environmental Sciences, University of Milano-Bicocca) provided helpful comments and suggestions on silicoflagellate morphology, while Luc Beaufort (CNRS-CEREGE, France) gave useful comments on microalgal biometric techniques. We are also indebted to Sumito Yamamoto (veteran of the Japan Maritime Self-Defense

Forces), who provided technical help on the debugging programme, test run, and useful subroutines of this morphometric programme, as well as giving strong encouragement throughout this study. This study was supported by research funds given to RWJ by Yamagata University. Finally, we would like to thank the two reviewers, Elisa Malinverno and Paulian Dumitrica, as well as the journal editor, Taniel Danelian, for their constructive comments, which greatly improved the paper.

Edited by: Taniel Danelian

Reviewed by: Elisa Malinverno and Paulian Dumitrica

## References

- Abe, K., McCartney, K., Fukunaga, Y., Narita, H., and Jordan, R. W.: Silicoflagellates and ebridians from the Seto Inland Sea and Kuroshio, including the description of *Octactis pulchra* var. *takahashii* var. nov., *Journal of Nannoplankton Research*, 35, 111–128, 2015.
- Benton, M. J., Csiki, Z., Grigorescu, D., Redelstorff, R., Sandder, P. M., Stein, K., and Weishampel, D. B.: Dinosaurs and the island rule: The dwarfed dinosaurs from Hațeg Island, *Palaeogeogr. Palaeoclimatol.*, 293, 438–454, 2010.
- Bukry, D. and Foster, J. H.: Silicoflagellate and diatom stratigraphy, Leg 16, Deep Sea Drilling Project, Initial Reports of the Deep Sea Drilling Project, 16, 815–871, 1973.
- Chang, F. H.: Cell morphology and life history of *Dictyochoa octonaria* (Dictyochophyceae, Ochrophyta) from Wellington Harbour, New Zealand, *Phycol. Res.*, 63, 253–264, 2015.
- Chiappe, L. M.: Downsized dinosaurs: The evolutionary transition to modern birds, *Evolution: Education and Outreach*, 2, 248–256, 2009.
- Cortese, G., Gersonde, R., Maschner, K., and Medley, P.: Glacial-interglacial size variability in the diatom *Fragilariopsis kerguelensis*: Possible iron/dust controls?, *Paleoceanography*, 27, PA1208, <https://doi.org/10.1029/2011PA002187>, 2012.
- Dumitrică, P.: *Silicoflagellate Miocene din Romania. Silicoflagellate miocene din Romania*, Teza de doctorat, Universitatea din București, Facultatea de Geologie-Geografie, București, 224 pp., 1974.
- Dumitrica, P.: Double skeletons of silicoflagellates: Their reciprocal position and taxonomical and paleobiological values, *Revue de micropaléontologie*, 57, 57–74, 2014.
- Gemeinhardt, K.: Silicoflagellatae, in: *Kryptogamen-Flora von Deutschland, Österreich und der Schweiz*, edited by: Rabenhorst, L., *Academische Verlagsgesellschaft*, Leipzig, 10, 1–87, 1930.
- Hanna, G. D.: Diatoms and silicoflagellates of the Kreyenhagen shale, California State of Mines Report, 27, 187–201, 1931.
- Henderiks, J. and Pagani, M.: Coccolithophore cell size and the Paleogene decline in atmospheric CO<sub>2</sub>, *Earth Planet. Sc. Lett.*, 269, 575–583, 2008.
- Henriksen, P., Knipschildt, F., Moestrup, Ø., and Thomsen, H. A.: Autecology, life history and toxicology of the silicoflagellate *Dictyochoa speculum* (Silicoflagellata, Dictyochophyceae), *Phycologia*, 32, 29–39, 1993.
- Ignatiades, L.: The relationship of the seasonality of silicoflagellates to certain environmental factors, *Bot. Mar.*, 13, 44–46, 1970.
- Kitchell, J. A.: Biotic interactions and siliceous marine phytoplankton: An ecological and evolutionary perspective. Biotic interactions in recent and fossil benthic communities, in: *Topics in Geobiology Series*, Vol. 3, edited by: Tevez, M. J. S. and McCall, P. L., *Plenum Publishing Corporation*, N.Y., 285–329, 1983.
- Loeblich, A. R., Loeblich, L., Tappan, H., and Loeblich Jr., A. R.: Annotated index of fossil and recent silicoflagellates and ebridians with descriptions and illustrations of validly proposed taxa, *The Geological Society of America, Inc., Memoir*, 106, 319 pp., 1968.
- Malinverno, E.: Extant morphotypes of *Distephanus speculum* (Silicoflagellata) from the Australian sector of the Southern Ocean: Morphology, morphometry and biogeography, *Mar. Micropaleontol.*, 77, 154–174, 2010.
- Malinverno, E., Karatsolis, B.-T., Dimiza, M. D., Lagaria, A., Psarra, S., and Triantaphyllou, M. V.: Extant silicoflagellates from the Northeast Aegean (eastern Mediterranean Sea): Morphologies and double skeletons, *Revue de micropaléontologie*, 59, 253–265, 2016.
- Marshall, S. M.: The Silicoflagellata and Tintinoidea, Great Barrier Reef Expedition 1928-29, *Scientific Reports*, 4, 623–634, 1934.
- McCartney, K., Witkowski, J., and Harwood, D. M.: Early evolution of the silicoflagellates during the Cretaceous, *Mar. Micropaleontol.*, 77, 83–100, 2010.
- McCartney, K., Witkowski, J., Jordan, R. W., Daugbjerg, N., Malinverno, E., van Wezel, R., Kano, H., Abe, K., Scott, F. J., Schweizer, M., Young, J. R., Hallegraeff, G. M., and Shiozawa, A.: Fine structure of silicoflagellate double skeletons, *Mar. Micropaleontol.*, 113, 10–19, 2014.
- McCartney, K., Abe, K., Harrison, M. A., Witkowski, J., Harwood, D. M., Jordan, R. W., and Kano, H.: Silicoflagellate double skeletons in the geologic record, *Mar. Micropaleontol.*, 117, 65–79, 2015.
- Onodera, J. and Takahashi, K.: Oceanographic conditions influencing silicoflagellate flux assemblages in the Bering Sea and subarctic Pacific Ocean during 1990–1994, *Deep-Sea Res. Pt. II*, 61–64, 4–16, 2012.
- Perch-Nielsen, K.: New silicoflagellates and a silicoflagellate zonation in north European Palaeocene and Eocene diatomites, *B. Geol. Soc. Denmark*, 25, 27–40, 1976.
- Perch-Nielsen, K.: Silicoflagellates, in: *Plankton stratigraphy*, Vol. 2, Radiolaria, diatoms, silicoflagellates, dinoflagellates and ichthyoliths, edited by: Bolli, H. M., Saunders, J. B., and Perch-Nielsen, K., *Cambridge University Press*, 811–846, 1985.
- Pérez-Méndez, N., Jordano, P., and Valido, A.: Downsized mutualisms: Consequences of seed disperses' body-size reduction for early plant recruitment, *Perspect. Plant Ecol.*, 17, 151–159, 2015.
- Poelchau, H. S.: Distribution of Holocene silicoflagellates in North Pacific sediments, *Micropaleontology*, 22, 164–193, 1976.
- Rigual-Hernández, A. S., Bárcena, M. A., Sierro, F. J., Flores, J. A., Hernández-Almeida, I., Sanchez-Vidal, A., Palanques, A., and Heussner, S.: Seasonal to interannual variability and geographic distribution of the silicoflagellate fluxes in the Western Mediterranean, *Mar. Micropaleontol.*, 77, 46–57, 2010.
- Rigual-Hernández, A. S., Trull, T. W., McCartney, K., Ballegeer, A.-M., Lawler, K.-A., Bray, S. G., and Armand, L. K.: Indices based on silicoflagellate assemblages offer potential for paleoreconstructions of the main oceanographic zones of the Southern Ocean, *Geo-Mar. Lett.*, <https://doi.org/10.1007/s00367-016-0444-8>, 2016.

- Shackell, N. L., Frank, K. T., Fisher, J. A. D., Petrie, B., and Leggett, C.: Decline in top predator body size and changing climate alter trophic structure in an oceanic ecosystem, *P. Roy. Soc. B-Biol. Sci.*, 277, 1353–1360, 2009.
- Shiono, M. and Jordan, R. W.: Recent diatoms of Lake Hibara, Fukushima Prefecture, *Diatom*, 11, 31–63, 1996.
- Suto, I.: The explosive diversification of the diatom genus *Chaetoceros* across the Eocene/Oligocene and Oligocene/Miocene boundaries in the Norwegian Sea, *Mar. Micropaleontol.*, 58, 259–269, 2006.
- Takeuchi, K.: Data analysis technique by SAS, 3rd Edn., University of Tokyo Press, 268 pp., 2011 (in Japanese).
- Tappan, H. N.: The paleobiology and plant protists, W. H. Freeman and Company, San Francisco, 1028 pp., 1980.
- Tsutsui, H. and Jordan, R. W.: A semi-automatic two-dimensional image system for studying the skeletal design of the silicoflagellate genus *Corbisema* (Dictyochales, Dictyochophyceae), *Journal of Nannoplankton Research*, 36, 1–9, 2016.
- Tsutsui, H. and Takahashi, K.: Biometry of *Distephanus medianocitoides* (Silicoflagellata) in the sea-ice covered environment of the central Arctic Ocean, summer 2004, *Memoirs of the Faculty of Science, Kyushu University, Series D, Earth Planetary Sciences*, 32, 57–68, 2009.
- Tsutsui, H., Takahashi, K., Nishida, S., and Nishiwaki, N.: Intraspecific morphological variation with biometry of *Distephanus speculum* (Silicoflagellata), *Mar. Micropaleontol.*, 72, 239–250, 2009.
- Tsuzaki, K.: Non mathematical statistics for medics, *Intuitive Biostatistics: A Nonmathematical Guide to Statistical Thinking*, 2nd Edn., edited by: Motulsky, H., 528 pp., 2011 (translated into Japanese).
- Young, J. R.: Size variation of Neogene *Reticulofenestra* coccoliths from Indian Ocean DSDP cores, *J. Micropaleontol.*, 9, 71–86, 1990.